PNAS RESEARCH ARTICLE | NEUROSCIENCE

BK channels mediate a presynaptic form of mGluR-LTD in the neonatal hippocampus

Carlos Ancatén-González[a,b], Rodrigo C. Meza[b], Naileth Gonzalez-Sanabria[a,b], Ignacio Segura[b], Alejandro Alcaino[a,b], Antonio Peña-Pichicoi[b], Ramón Latorre[b], Chiayu Q. Chiu[b], and Andrés E. Chávez[b,1]

Affiliations are included on p. 8.

Edited by Julie Kauer, Stanford University, Stanford, CA; received June 20, 2024; accepted December 7, 2024 by Editorial Board Member Carol A. Mason

BK channels can control neuronal function, but their functional relevance in activity-dependent changes of synaptic function remains elusive. Here, we report that repetitive low-frequency stimulation activates BK channels through 12(S)HPETE, an arachidonic acid metabolite, produced downstream of postsynaptic metabotropic glutamate receptors (mGluRs) to trigger long-term depression (LTD) at CA3–CA1 synapses in hippocampal slices from P7–P10 mice. Activation of BK channels is subunit specific, as paxilline but not iberiotoxin blocked mGluR-LTD. Also, 12(S)HPETE does not change the electrophysiological properties of the BK channel when the BKα subunit is expressed alone but increases the channel open probability when the BKα is coexpressed with the β4-subunit. Our findings reveal an interaction between 12(S)HPETE and BK channels to regulate synaptic strength at central synapses and increase our understanding of the mechanisms underlying mGluR-LTD in the neonatal hippocampus that likely contribute to circuit maturation necessary for learning.

retrograde signaling | synaptic plasticity | BK channels | hippocampus

Activity-dependent long-term depression (LTD) of excitatory synaptic strength contributes to circuit remodeling and memory formation. Although with varying mechanisms depending upon brain region and developmental progress, a common cellular mechanism for LTD is the reliance on postsynaptic activation of group I metabotropic glutamate receptors (mGluRs) to induce either pre- or postsynaptic forms of mGluR-LTD (1). In the hippocampus, neonatal LTD is known to require mGluRs to subsequently generate a lipid-derived metabolite from arachidonic acid, known as 12(S)HPETE. Once produced, 12(S)HPETE travels retrogradely to the CA3 axon terminal to suppress glutamate release onto CA1 pyramidal neurons in a long-term manner (2–4). However, the precise downstream targets of 12(S)HPETE at presynaptic sites involved in this form of mGluR-LTD remain elusive.

Lipid derivates, including the lipoxygenase-derived 12(S)HPETE, represent one of the primary activating ligands of TRP channels (5, 6). For instance, 12(S)HPETE-dependent LTD in the mature hippocampus has been reported at glutamatergic synapses onto CA1 inhibitory interneurons. This form of plasticity involves the activation of the presynaptic transient potential vanilloid 1 receptor (TRPV1) (7). Whether TRPV1 channels are also a key player in neonatal mGluR-LTD at CA3-CA1 excitatory synapses remains unknown. Apart from their action on TRP receptors, lipid derivates are also known to modulate synaptic efficacy by directly acting on voltage-gated ion channels (8), including calcium (9) and potassium channels (10, 11). Interestingly, the large-conductance, calcium- and voltage-activated potassium channels (BK), known to regulate neuronal excitability and synaptic function throughout the brain (12, 13), are reportedly regulated by different lipoxygenase-derived metabolites (14, 15). Moreover, evidence indicates that BK channels are expressed at presynaptic terminals of CA3 neurons in the mature hippocampus (16–19), opening the possibility that BK channels are involved in mGluR-LTD. However, whether presynaptic BK channels contribute to neonatal activity-dependent mGluR-LTD remains unknown.

Here, using electrophysiological recordings in acute hippocampal slices from P7–P10 mice, we evaluate the role of TRPV1 and BK channels as potential downstream effectors of 12(S)HPETE signaling in mediating neonatal mGluR-LTD. We find that activation of presumably presynaptic BK, but not TRPV1, channels by 12(S)HPETE is required for the induction of mGluR-LTD at immature CA3–CA1 synapses. The contribution of BK channels is subunit specific, involving BK containing β4 but not β2 subunit. These results identify a mechanistically necessary step for the induction of mGluR-LTD during postnatal

Significance

Calcium- and voltage-activated potassium channels (BK) are well known to regulate neuronal excitability and synaptic function throughout the brain. However, the contribution of BK channels to activity-dependent changes of synaptic efficacy remains elusive. Here, we report that an arachidonic acid–derived metabolite activates BK channels to induce long-term depression of glutamate release mediated by metabotropic glutamate receptor (mGluR-LTD) in the neonatal hippocampus. This modulation of synaptic efficacy is subunit specific, as BK channels containing the β4 but not β2 subunit are required. These results highlight the contribution of BK channels in activity-dependent regulation of synaptic efficacy and identify a subunit-dependent activation of BK channels by lipid messengers to regulate synaptic function in a long-term manner in the neonatal hippocampus.

Author contributions: C.A.-G., R.L., C.Q.C., and A.E.C. designed research; C.A.-G., R.C.M., N.G.-S., I.S., A.A., and A.P.-P. performed research; R.L. and A.E.C. contributed new reagents/analytic tools; C.A.-G., R.C.M., N.G.-S., I.S., A.A., A.P., C.Q.C., and A.E.C. analyzed data; and C.A.-G., R.L., C.Q.C., and A.E.C. wrote the paper.

The authors declare no competing interest.

This article is a PNAS Direct Submission. J.K. is a guest editor invited by the Editorial Board.

[1]To whom correspondence may be addressed. Email: andres.chavez@uv.cl.

This article contains supporting information online at https://www.pnas.org/lookup/suppl/doi:10.1073/pnas.2411506122/-/DCSupplemental.

Published January 8, 2025.

development that likely involves retrograde activation of BK channels at presynaptic terminals to impact synaptic function in a long-term manner.

Results

12(S)HPETE Is a Key Player of Presynaptic mGluR-LTD in the Neonatal Hippocampus. To investigate the presynaptic mechanisms involved in the induction of mGluR-LTD, we recorded field excitatory postsynaptic potentials (fEPSPs) and currents (EPSCs) from CA1 pyramidal neurons while stimulating CA3 Schaffer collateral inputs in acute hippocampal slices of neonatal (postnatal day P7–P10) mice (*Materials and Methods*). Consistent with previous reports (2, 3, 20, 21), low-frequency stimulation (LFS, 5 Hz, 3 min) induced a robust LTD that required postsynaptic mGluRs as it was eliminated by the mGluR5 antagonist MTEP (10 μM, Fig. 1*A*). Moreover, LFS-induced LTD can also be abolished by loading CA1 pyramidal neurons with GDPβS, a broad-spectrum G protein antagonist but was normally induced when NMDA receptors were blocked with APV (*SI Appendix*, Fig. S1 *A–C*). LFS-induced LTD was also independent of GABAergic transmission as it was normally induced in the presence (Fig. 1*A*) or absence of the $GABA_A$ receptor antagonist picrotoxin (50 μM; *SI Appendix*, Fig. S1*B*). Similarly, mGluR-LTD could be mimicked by pharmacological activation of mGluRs with DHPG (50 μM, 10 min), an effect that was also eliminated in the continuous presence of MTEP (Fig. 1*B*). Importantly, both electrical and chemical forms of mGluR-LTD were accompanied by changes in the paired-pulse ratio (PPR) and coefficient of variation ($1/CV^2$; Fig. 1 *A* and *B*), consistent with a presynaptic origin. Moreover,

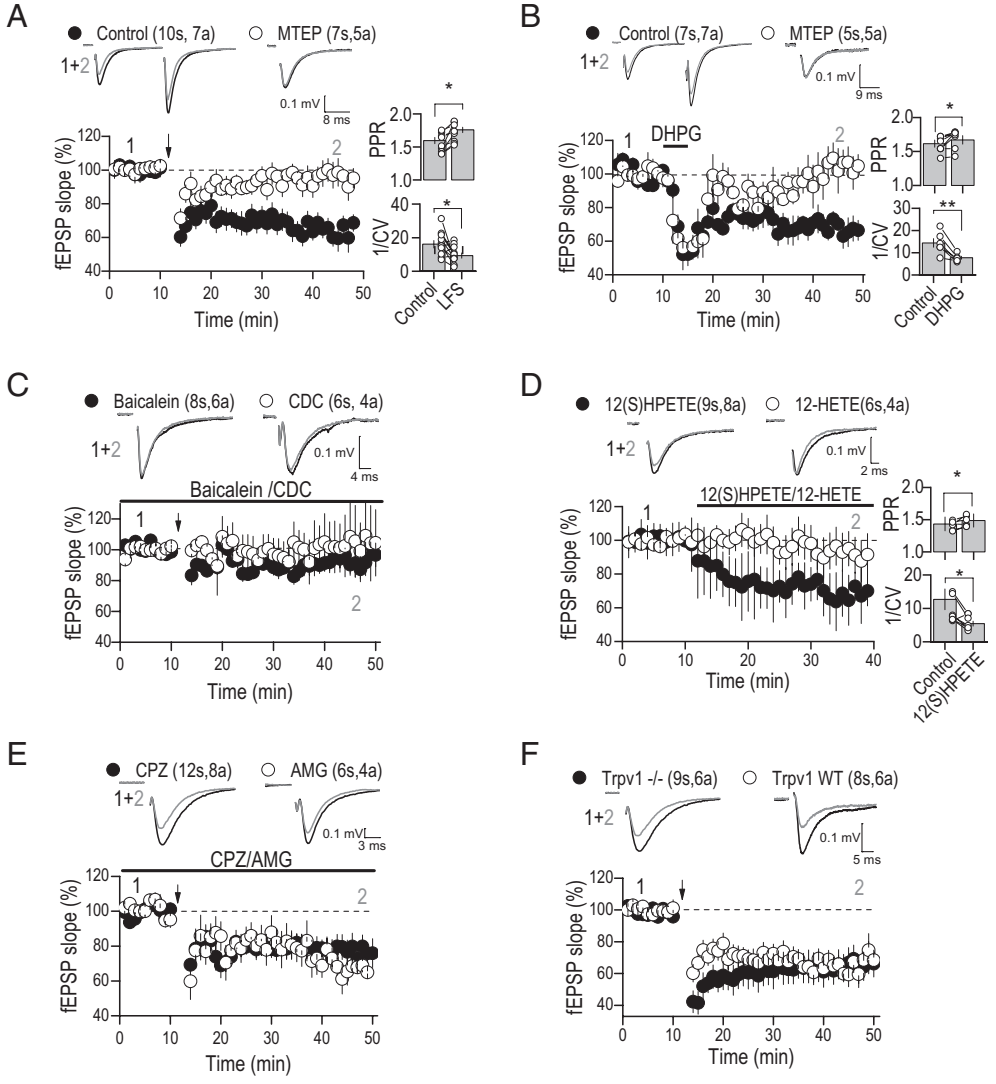

Fig. 1. Arachidonic acid metabolite 12(S)HPETE is necessary to induce mGluR-LTD in the young hippocampus. (*A*) Low-frequency stimulation (LFS, 5 Hz, 3 min) induces a LTD of fEPSP (black circle) that was eliminated in the continuous presence of the mGluR antagonist MTEP (10 μM; open circle). *Top,* Representative traces of two consecutive fEPSP (100-ms interstimulus interval) before (black) and after (grey) LFS induction, and in the continuous presence of MTEP. *Bottom*, summarized graphs. (*B*) Representative traces (*Top*) and time course (*Bottom*) showing that bath application of the mGluR agonist DHPG (50 μM, 5 min) also induces LTD of fEPSP, an effect that was eliminated in the continuous presence of MTEP. Note that LFS- and DHPG-induced mGluR-LTD were accompanied by changes in PPR and coefficient of variation ($1/CV^2$, *Right*), suggesting a presynaptic mechanism involved. In the PPR and $1/CV^2$ summarized plot, each open circle represents a single slice. (*C*) Representative traces (*Top*) and time course (*Bottom*) showing that blocking 12-lypoxigenase, and the production of 12(S)HPETE with two independent blockers (Baicalein and CDC), eliminates LFS-induced LTD. (*D*) Representative traces (*Top*) and time course (*Bottom*) showing that 12(S) HPETE (100 nM), but not its metabolite 12-HETE (100 nM), reduced fEPSP at CA3-CA1 synapses, an effect that was accompanied by changes in PPR and $1/CV^2$. (*E*) Representative traces (*Top*) and time course (*Bottom*) showing that LFS-induced mGluR-LTD was unaffected by two different TRPV1 antagonists Capsazepine (CPZ, 10 μM) and AMG 9810 (AMG, 10 μM). (*F*) Representative traces (*Top*) and time course (*Bottom*) showing that LFS-induced mGluR-LTD is similar in wild-type ($TRPV1^{+/+}$) and $TRPV1^{-/-}$ deficient mice. In all panels, data are presented as mean ± SEM, and averaged sample traces taken at times indicated by numbers are shown next to each summary plot. **P* <0.05, ***P* <0.01, and the number of slices (s) and animals (a) are indicated in parenthesis.

LFS- and DHPG-induced LTD occluded each other (*SI Appendix*, Fig. S1 *D* and *E*), indicating that mGluR activation by either pharmacological means or synaptic activity suppresses glutamate release in the young hippocampus through a common presynaptic mechanism.

Previous evidence indicates that presynaptic mGluR-LTD requires a postsynaptic signal pathway that involves the activation of 12-lipoxygenase and the production of the lipid metabolite 12(S) HPETE (2, 4, 22). Accordingly, two independent 12-lipoxygenase inhibitors, baicalein (10 μM) and cinnamyl-3,4-dihydroxy-α-cyanocinnamate (CDC; 10 μM), were able to eliminate both LFS- (Fig. 1*C*) and DHPG-induced mGluR-LTD (*SI Appendix*, Fig. S1*F*). Moreover, bath application of 12(S)HPETE (100 nM), but not its metabolite 12-HETE (100 nM), was sufficient to reduce fEPSPs in a long-lasting manner in the young hippocampus (Fig. 1*D*). Consistent with a presynaptic mechanism, 12(S)HPETE-mediated synaptic depression was accompanied by changes in PPR and $1/CV^2$ (Fig. 1*D*) and occluded the induction of either LFS- or DHPG-induced mGluR-LTD (*SI Appendix*, Fig. S2 *A* and *B*). Moreover, 12(S)HPETE had no further effect on fEPSP amplitude if applied after the induction of LFS-LTD (*SI Appendix*, Fig. S2*C*). Altogether, these results strongly support the idea that 12(S)HPETE is a key player in the induction of presynaptic mGluR-LTD in the neonatal hippocampus (2).

mGluR-LTD at CA3-CA1 Synapses Does Not Involve the Activation of TRPV1 Channels. What is the potential target of 12(S)HPETE at presynaptic terminals to induce mGluR-LTD? In the mature hippocampus, at excitatory CA3 to interneuron synapses, mGluR-LTD reportedly requires activation of presynaptic TRPV1 channels (7). However, LFS-induced mGluR-LTD at immature CA3 to CA1 synapses was normally induced when TRPV1 channels were blocked with capsazepine (CPZ, 10 μM) or AMG 9810 (AMG; 10 μM Fig. 1*E*) or in slices from TRPV1 deficient mice ($TRPV1^{-/-}$; Fig. 1*F*), further supporting that, unlike the excitatory CA3 to interneuron synapse (7), TRPV1 channels are not involved in presynaptic mGluR-LTD mediated by 12(S)HPETE at excitatory CA3-CA1 synapses in the neonatal hippocampus. Consistent with this idea, 12(S)HPETE markedly reduced fEPSPs in the continuous presence of CPZ or AMG (*SI Appendix*, Fig. S3*A*) or in hippocampal slices from $TRPV1^{-/-}$ mice (*SI Appendix*, Fig. S3*B*), strongly suggesting that TRPV1 channels are not required for 12(S)HPETE-mediated depression in the young hippocampus. Accordingly, bath application of capsaicin (1 μM), a TRPV1 agonist, had no significant effect on basal synaptic transmission at CA3-CA1 excitatory synapses (*SI Appendix*, Fig. S3*C*), but depressed the CA3-interneuron synapse in naïve slices (*SI Appendix*, Fig. S3*C*).

BK Channels Are Required for the Induction of mGluR-LTD in the Neonatal Hippocampus. Previous evidence suggests that BK channels regulate synaptic transmission at CA3 axon terminals (16, 18) and can be regulated by different lipoxygenase-derived metabolites (14, 15), but whether they play a role in regulating mGluR-LTD remains unknown. To assess their involvement in mGluR-LTD, we first applied BK channel antagonists before delivering LFS- or DHPG to induce mGluR-LTD. Blocking BK channels with iberiotoxin (100 nM) had no effect on electrical and chemical forms of mGluR-LTD (Fig. 2 *A* and *B*). However, bath application of the BK channel antagonist paxilline (1 or 10 μM) was able to abolish both forms of LTD (Fig. 2 *A* and *B*). For completeness, we also performed experiments using apamin, a blocker of the small-conductance voltage- and Ca^{2+}-sensitive potassium (SK) channels known to regulate synaptic plasticity in the adult hippocampus (23). While apamin (300 nM) was able to reduce medium afterhyperpolarization current (I_{mAHP}) in CA1 pyramidal neurons, it failed to block LFS-induced mGluR-LTD (*SI Appendix*, Fig. S4 *A* and *B*). Thus, our results suggest that paxilline-sensitive BK channels are involved in mGluR-LTD. Accordingly, paxilline but not iberiotoxin eliminated 12(S) HPETE-induced depression of synaptic transmission (Fig. 2*C*). Importantly, paxilline had no effect on basal synaptic transmission (*SI Appendix*, Fig. S4*C*) or in synapses already expressing 12(S) HPETE-mediated depression (*SI Appendix*, Fig. S4*D*) and LFS-induced LTD was normally expressed when paxilline was applied immediately after tetanus (*SI Appendix*, Fig. S4*E*), suggesting that paxilline-sensitive BK channels are required for the induction, but not maintenance of mGluR-LTD. Moreover, bath application of the specific BK channel agonist NS11021 (3 μM) was sufficient to reduce basal synaptic transmission at CA3-CA1 synapses (Fig. 2*D*). This effect was accompanied by changes in PPR and $1/CV^2$ and was eliminated in slices preincubated with paxilline but not with iberiotoxin (Fig. 2*D*). Moreover, a short application of NS11021 (5 min) also induces a long-lasting and irreversible reduction of fEPSP (*SI Appendix*, Fig. S4*F*). Consistent with the idea that paxilline-sensitive BK channels are required for the induction, but not maintenance of synaptic depression at CA3-CA1 synapses, paxilline had no effect on synapses already expressing NS11021-mediated depression (*SI Appendix*, Fig. S4*G*). Moreover, in the continuous presence of NS11021, LFS and DHPG were not able to further suppress fEPSPs (Fig. 2*E*). Importantly, NS11021-mediated depression could not be induced at synapses already expressing 12(S)HPETE-mediated depression (Fig. 2*F*). Inversely, 12(S)HPETE had no effect on synapses already expressing NS11021-mediated depression (Fig. 2*F*). These two-way occlusion experiments indicate that 12(S)HPETE- and NS11021-mediated synaptic depression share a common mechanistic step to induce mGluR-LTD. To explore this possibility, we delivered a subthreshold induction protocol, which by itself did not have persistent effects on fEPSPs (*SI Appendix*, Fig. S5*A*) and did not occlude further induction of LFS-LTD (*SI Appendix*, Fig. S5*B*). We tested whether such a protocol could be potentiated to trigger LTD by slightly elevating BK channel activity with the use of brief application of BK agonists 12(S)HPETE or NS11021, which does not by itself produce lasting suppression. Under these recording conditions, the subthreshold induction protocol triggered robust LTD that was blocked by paxilline (*SI Appendix*, Fig. S5 *C* and *D*). Altogether, these results support the idea that paxilline-sensitive BK channel activation is necessary to induce mGluR-LTD in the young hippocampus.

The BK Channel Containing β4 but not the β2 Subunit Is Sensitive to 12(S)HPETE. The differential effect between iberiotoxin and paxilline on mGluR-LTD, and 12(S)HPETE- and NS11021-mediated depression, suggests that BK channels containing β4 but not β2 subunits are required for this form of LTD. To further investigate this possibility, we tested the effect of 12(S)HPETE on human BK channels formed by the α, the α+ β2, and α+ β4 subunits expressed in *Xenopus laevis* oocytes. Notably, 12(S) HPETE does not change the BK channel voltage dependence when the BKα subunit is expressed alone (Fig. 3*A*), but strongly increases the channel open probability when the β4-subunit was coexpressed with the α subunit (Fig. 3*B*). The addition of 12(S)HPETE intracellularly to a final concentration of 100 nM produces a 50 mV leftward shift of the normalized BKβ4 channel open probability ($I_{tail}/I_{tailmax}$)-voltage curve (Fig. 3*B*). The half voltages obtained from the $I_{tail}/I_{tailmax}$ vs voltage curves were plotted against 12(S)HPETE concentration, and the data were

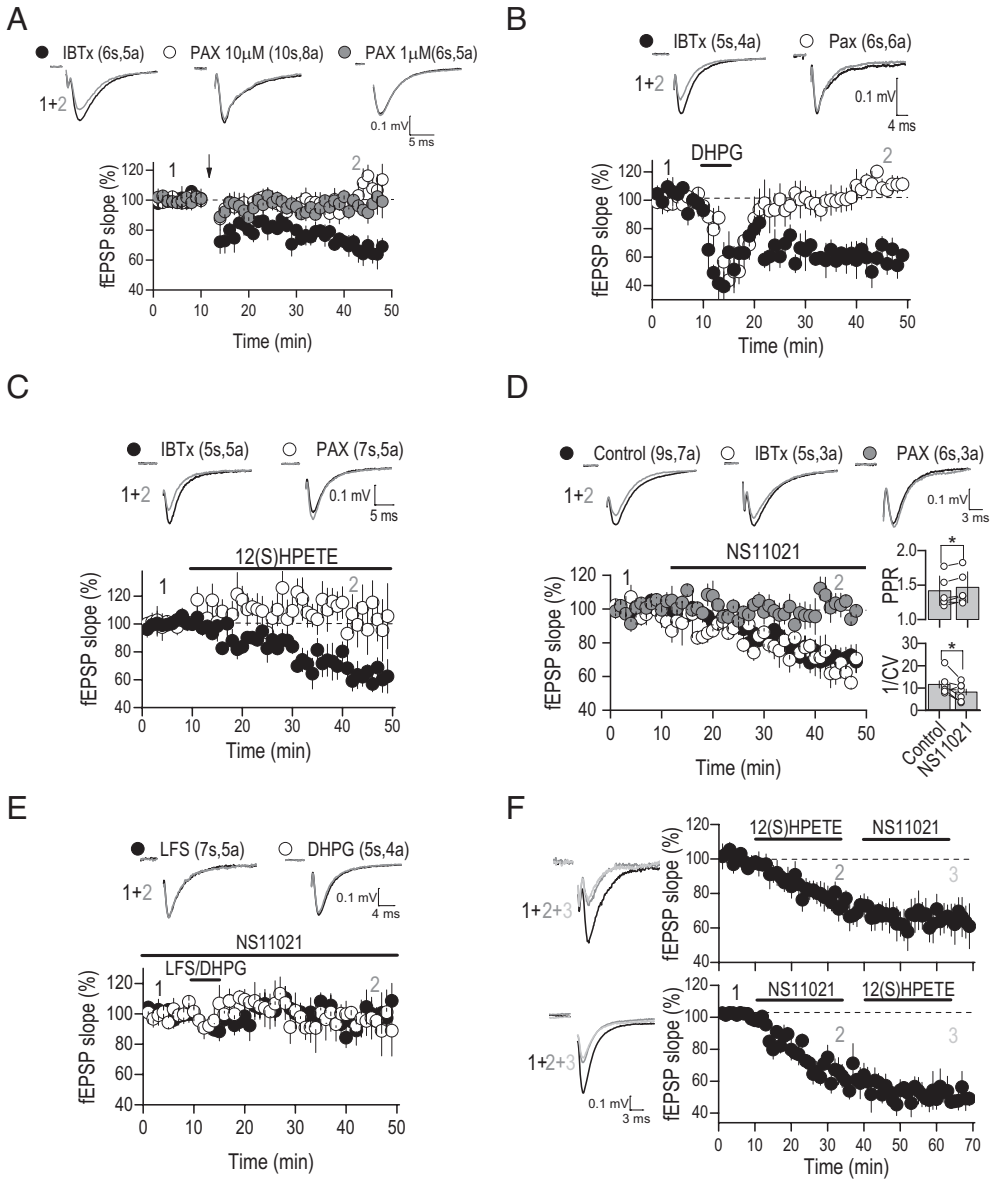

Fig. 2. Activation of BK channels containing the BKβ4 subunit is involved in mGluR-LTD. (*A*) Average traces (*Top*) and time course (*Bottom*) showing that LFS- and (*B*) DHPG-induced mGluR-LTD were unaffected by bath application of iberiotoxin (IBTx, 100 nM) but were eliminated in the continuous presence of Paxilline (Pax, 10 or 1 μM). (*C*) Average traces (*Top*) and time course (*Bottom*) showing that bath application of the 12(S)HPETE (100 nM) depresses fEPSP in the continuous presence of IBTx but had no effect in the presence of Pax. (*D*) Average traces (*Top*) and time course (*Bottom*) showing that bath application of NS11021 (3 μM), a BK channel agonist, depresses fEPSP in the continuous presence of IBTx but had no effect in the presence of Pax. NS1121-mediated depression of fEPSP was accompanied by changes in PPR and 1/CV, suggesting a presynaptic mechanism of action. (*E*) Average traces (*Top*) and time course (*Bottom*) showing that preincubation with NS11021 (3 μM) is able to block LFS- and DHPG-induced mGluR-LTD. (*F*) Average traces (*Left*) and time course (*Right*) showing that 12(S)HPETE-induced suppression of fEPSP occluded the NS11021-mediated depression of fEPSP at CA3-CA1 synapses (*Top*), and inversely, NS11021-induced depression blocks further effect of 12(S)HPETE (*Bottom*), suggesting a common mechanism of action. In all panels, data are presented as mean ± SEM, and averaged sample traces taken at times indicated by numbers are shown next to each summary plot, and the numbers of slices (s) and animals (a) are indicated in parentheses. *$P < 0.05$

fitted using a Hill equation (see legend of Fig. 3*C*). The best fit to the data was obtained with a dissociation constant of 0.98 nM and a Hill coefficient of 3 (Fig. 3*C*). Demonstrating that the effect of 12(S)HPETE is subunit specific, this metabolite did not modify the voltage dependence of α + β2 channels (Fig. 3*D*). Importantly, 12(S)HPETE-mediated effect in BKβ4 channel open probability is amplified by internal Ca^{2+} given that in the presence of 3 μM internal Ca^{2+}, the probability of opening-voltage curve shifted leftward by 77 mV, twice the effect observed in the absence of internal Ca^{2+} (Fig. 3*E*). Moreover, cytoplasmic Ca^{2+} does not affect the binding of 12(S)HPETE to the BK channel as the equilibrium dissociation constant is close to 1 nM (Fig. 3*F*). These results support the idea that BK channels formed by α and β4 subunits, but not β2-subunits, are necessary for the induction of 12(S)HPETE-mediated depression and mGluR-LTD in the young hippocampus and a tight binding accompanies this subunit specificity.

Presynaptic BKβ4 Channels Likely Regulate CA3-CA1 Synapses and mGluR-LTD. Although BK channels are expressed in pre- and postsynaptic compartments in the hippocampus (12, 16, 18, 19, 24, 25) and its inhibition with either paxilline and iberiotoxin can regulate the excitability of CA1 pyramidal neurons (*SI Appendix*, Fig. S6), the changes in PPR and $1/CV^2$ that we observed after the induction of 12(S)HPETE- and NS11021-mediated depression as well as in mGluR-LTD (Figs. 1–3) suggest that presynaptic rather than postsynaptic BK channels are necessary for the induction of mGluR-LTD. Consistent with this idea, BKβ4 channel

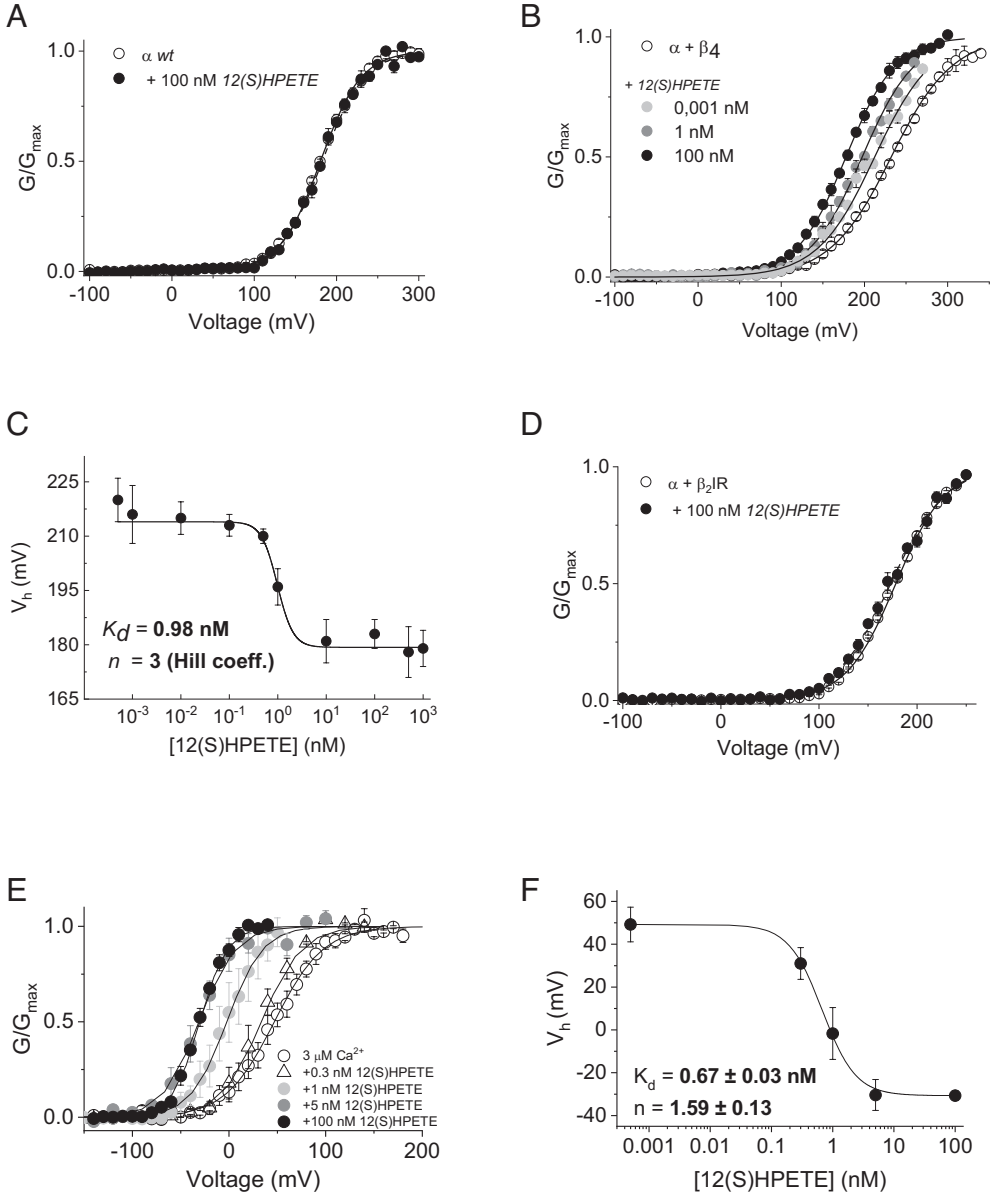

Fig. 3. BK channels containing β4 but not β2 subunit are directly activated by 12(S)HPETE. (*A*) Normalized I_{tail}-V relationship ($I_{tail}(V)$) for BK α channels before (white diamonds) or after (black diamonds) the addition of 12(S)HPETE (100 nM) to the cytoplasmic side in 0 $[Ca^{2+}]_i$. The I_{tail}(V) data (mean ± SEM) were fitted using a Boltzmann function (*Materials and Methods*). Fit parameters were V_h = 180 and 182 mV; z_δ = 1.02 and 0.98 before (n = 5) and after (n = 5) the addition of 12(S)HPETE, respectively. (*B*) Normalized $I_{tail}(V)$ (mean ± SEM) for BK $\alpha + \beta_4$ channels before (white hexagons) or after the addition of 12(S)HPETE at concentrations of 0.001 nM (black squares); 1 nM (black circles) or 100 nM (black triangles) to the internal side. Fit parameters were V_h = 233 mV and z_δ = 0.69, n = 7 (control); V_h = 217 mV and z_δ = 0.78, n = 4 (0.001 nM); V_h = 196 mV and z_δ = 0.81, n = 4 (1 nM); and V_h = 183 mV and z_δ = 0.76, n = 5 (100 nM). (*C*) Average V_h values obtained from the $I_{tail}(V)$ curves plotted against 12(S)HPETE concentration (mean ± SEM). Data were fitted using a Hill equation where $V_h = V_{max} + \frac{(V_0 - V_{max}) \times [HPETE]^n}{K^n + [HPETE]^n}$ where V_{max} is the half voltage in the absence of 12(S)HPETE, V_o is the half voltage at the indicated 12(S)HPETE concentration, K the dissociation constant, and n the Hill coefficient. 12(S)HPETE binding produces a leftward shift in V_h (ΔV_h) (n = 3 to 4). (*D*) Normalized I_{tail}-V (mean ± SEM) for BK $\alpha + \beta_2$IR channels before (white diamonds) or after (black diamonds) the addition of 100 nM 12(S)HPETE to the cytoplasmic side in 0 $[Ca^{2+}]_i$. Fit parameters were V_h = 178 and 174 mV; z_δ = 0.99 and 0.90 before (n = 4) and after (n = 4) the addition of 12(S)HPETE, respectively. (*E*) Normalized $I_{tail}(V)$ (mean ± SEM) for BK α + β4 channels, in the presence of 3 μM of Ca^{+2}, before (open circles) or after the addition of 12(S)HPETE at different concentrations. Data were fitted using a Boltzmann equation (*Materials and Methods*). The parameters were before the addition of 12(S)HPETE: V_h = 46.86 ± 1.12 mV, and zδ = 1.00 ± 0.04 e_0 (n = 3); 0.3 nM: V_h = 33.34 ± 1.31 mV, and zδ = 1.1 ± 0.06 e_0 (n = 3); 1 nM: V = −2.33 ± 1.25 mV, and zδ = 1.36 ± 006 (n = 3); 5 nM: V_h = −31.18 ± 1.99 mV, and zδ = 1.34 ± 0.12 (n = 3); 100 nM (n = 4): V = −30.33 ± 0.56 mV, and zδ = 1.77 ± 0.06 (n = 4). (*F*) Average V_h values obtained from the I_{tail}(V) curves plotted against 12(S)HPETE concentration (mean ± SEM) in the presence of 3 μM of Ca^{+2}. The V_{half} −[12(S)HPETE] data were fitted to a Hill equation as described in Fig. 3*C*.

activation by bath application of the agonist NS11021 or 12(S)HPETE has no effect on CA1 responses elicited by brief puffs of glutamate (monitored at −60 mV), a manipulation known to shortcut glutamate release (Fig. 4*A*). Moreover, bath application of the BK channel agonist NS11021 depressed isolated NMDA receptor (NMDAR)-mediated EPSCs (*Materials and Methods*) to an extent similar to that of AMPAR-mediated fEPSPs (Fig. 2*C*), consistent with a decrease in glutamate release (Fig. 4*B*). Additional observations further support a presynaptic localization of BKβ4 to regulate synaptic plasticity. First, when EPSCs and fast afterhyperpolarization current (I_{fAHP}) were recorded from the same CA1 pyramidal neuron, bath application of 12(S)HPETE induced depression of EPSC but had no effect on postsynaptic I_{fAHP} (Fig. 4*C*). Second, 12(S)HPETE-induced LTD was associated with an increase in failure rate in minimal stimulation experiments (Fig. 4*D*), an effect that was eliminated in the continuous presence

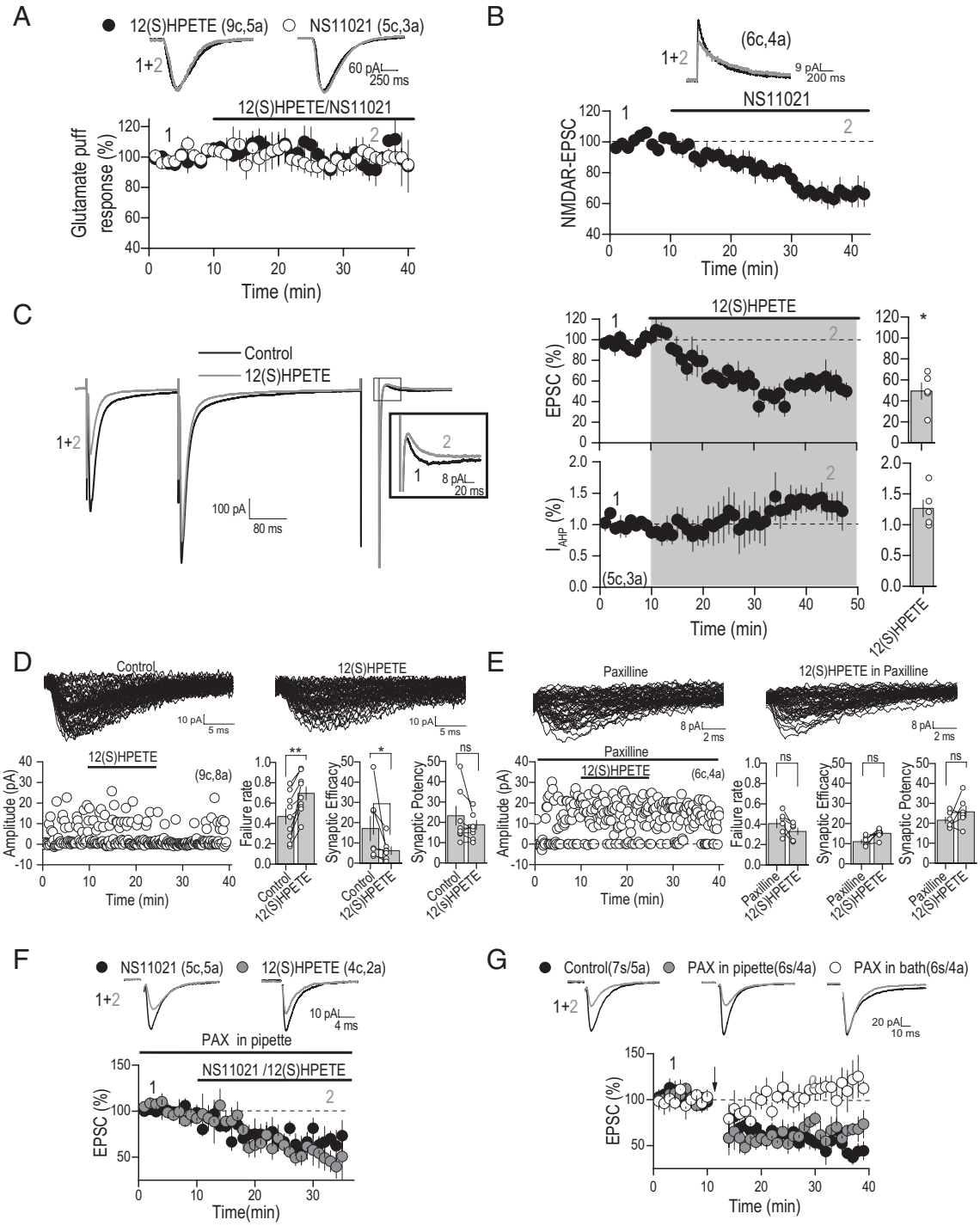

Fig. 4. Activation of BKβ4 is required for mGluR-LTD. (*A*) Average traces (*Top*) and time course (*Bottom*) showing that postsynaptic response to exogenous glutamate puff application (1 mM, 25 ms) was unaffected by bath application of BK channels agonist 12(S)HPETE (100 nM) and NS11021 (3 μM). (*B*) Average trace (*Top*) and time course (*Bottom*) showing that NS11021 induces a depression of isolated NMDAR-mediated currents in a similar way as to AMPAR-mediated currents. (*C*) Average trace (*Left*) and summarized graph (*Right*) showing that 12(S)HPETE (100 nM) decrease presynaptic neurotransmission (EPSC; *Top*) without affecting postsynaptic excitability (I_{fAHP}; *Bottom*) recorded at the same time from neonatal CA1 pyramidal neuron. (*D*) Individual traces (*Top*) and summarized graphs (*Bottom*) showing that 12(S)HPETE (100 nM) increased failure rate and decreased synaptic efficacy but had no effect on synaptic potency of minimal stimulation experiments in the CA1 area of the hippocampus, supporting a presynaptic mechanism of action. (*E*) Individual traces (*Top*) and time course (*Bottom*) showing that bath application of paxilline (10 μM) eliminated 12(S)HPETE-mediated increase in failure rate and decrease in synaptic efficacy, supporting that 12(S)HPETE effect is mediated by presynaptic BKβ4 channels. (*F*) Representative traces (*Top*) and time course (*Bottom*) showing that loading CA1 pyramidal neuron with paxilline (Pax; 10 μM) was not able to block NS11021- and 12(S)HPETE-induced synaptic depression. (*G*) Representative traces (*Top*) and time course (*Bottom*) showing that Pax in bath, but not intracellularly applied, is able to block LFS-induced LTD in the neonatal hippocampus. In all panels, data are presented as mean ± SEM, and averaged sample traces taken at times indicated by numbers are shown next to each summary plot and the numbers of cells (c) and animals (a) are indicated in parentheses. ns, no significant; * $P < 0.05$, ** $P < 0.01$.

of paxilline (Fig. 4*E*). Third, loading CA1 pyramidal cells with the BK channel blocker paxilline through the patch pipette, a manipulation known to reduce the excitability of CA1 pyramidal neurons (26, 27) (*SI Appendix*, Fig. S6 *A–C*), does not affect synaptic depression induced by either NS11021 or 12(S)HPETE (Fig. 4*F* and *SI Appendix*, Fig. S6*D*). Additionally, bath-applied

paxilline abolished LFS-induced mGluR-LTD, but intracellularly loaded paxilline (Fig. 4*G*) or cesium to block BK channels failed to prevent LTD (*SI Appendix*, Fig. S6*E*). Altogether, these results strongly suggest that presynaptic rather than postsynaptic BK channels are necessary for the induction of mGluR-LTD.

Discussion

Our findings reveal that BKβ4 channels are a crucial substrate involved in classical mGluR-LTD in the neonatal hippocampus and identify a form of lipids-derived retrograde modulation of synaptic function that involves an interaction between 12(S)HPETE and BK channels at central synapses. Notably, this modulation of synaptic strength mediated by BK channels is subunit specific as BKβ4, but not BKβ2, is activated in an activity-dependent manner to depress in a long-term manner CA3-CA1 excitatory synaptic transmission in the young hippocampus.

Multiple forms of retrograde signaling mediated by lipid messengers, including endocannabinoids and endovanilloids/eicosanoids, are known to modulate synaptic function and plasticity at central synapses, mainly by activating CB1 and TRPV1 receptors, respectively (28, 29). Now, we add to this repertoire that the lipoxygenase product from arachidonic acid, 12(S)HPETE, can directly bind and activate presumably presynaptic BK channels containing β4 subunit generating a long-lasting depression of transmitter release at CA3-CA1 excitatory synapses in the young hippocampus (*SI Appendix*, Fig. S7). Thus, our data, together with those indicating that retrograde regulation of potassium channels by arachidonic acid metabolites regulate synaptic plasticity at the CA3 area of the hippocampus (11), support the idea that lipid-derived metabolites and potassium channels interaction might play an important role in the mechanisms underlying hippocampal synaptic plasticity. An additional observation of our results is the input-specific effect of the retrograde modulation mediated by 12(S)HPETE in the hippocampus. While at excitatory CA3 to interneuron synapses, 12(S)HPETE acts through TRPV1 channels to regulate synaptic plasticity (7), our results demonstrated that at excitatory CA3-CA1 synapses BKβ4, but not TRPV1 channels are required to regulate synaptic plasticity. The differential reliance on BKβ4 versus TRPV1 depending on whether the postsynaptic target is pyramidal versus interneurons suggests that CA3 axon terminals may express specific receptor subtypes depending on the postsynaptic partner (*SI Appendix*, Fig. S3*C*). In addition, it is also unclear whether the retrograde modulation mediated by 12(S)HPETE could also be expressed at other synapse types within the neonatal brain and in the adult hippocampus. Interestingly, a functional interaction between TRPV1 and BK channels has been suggested in the peripheral nervous system (30). Whether this functional interaction also regulates central synapses remains unclear, and further investigation is necessary to understand when and how retrograde modulation by 12(S)HPETE regulates synaptic function through TRPV1 or BKβ4 channels.

Consistent with a retrograde modulation of synaptic function, we demonstrated that 12(S)HPETE acts on presynaptic BK channels (Fig. 4) despite their expression in postsynaptic compartments where they are known to regulate neuronal excitability (24, 31). While the differential activation of pre- vs postsynaptic BK channels by this lipid-derived remains unclear, it could be due to different β-subunits expressed in both neuronal compartments. For instance, it has been proposed that β4 subunits are present in CA3 pyramidal neurons (32, 33) and dentate granule cells in the dentate gyrus (24), whereas β2 are present in CA1 pyramidal neurons (34). Moreover, some reports indicate that subtypes of the BK channel, depending on their β subunits, can be differentially activated by lipids (35, 36) and also some hormones (37). Consistent with this idea, our results using heterologous expression demonstrate that BKβ4, but not a- and or BKβ2 channel, is directly modulated by 12(S)HPETE. Moreover, 12(S)HPETE-mediated retrograde suppression of synaptic function was blocked by paxilline but not by iberiotoxin, which blocks BKβ2 and aBK but not BKβ4 channels. Interestingly, at mature hippocampal synapses, the role of presynaptic BK channels can only be unmasked by blocking Kv channels and BK channels become sensitive to iberiotoxin (16), opening the possibility that developmental changes in the expression or quantity of β4 subunits may occur at presynaptic terminals during postnatal development to regulate synaptic function.

BK channels have been involved in some forms of short-term plasticity (32, 38), and our present results demonstrated its involvement in long-lasting depression in the neonatal hippocampus. While the exact mechanisms by which BK channels can generate a LTD vs a short-term plasticity is unknown, it is possible that the localization of BKβ4 at the presynaptic nerve terminal likely modulates both the amplitude and duration of depolarization evoked calcium influx limiting vesicle fusion at active zones and decreased neurotransmitter release (16, 18) in a long-term manner. It is also possible that changes in kinase/phosphatase balance downstream of BK activation might also be involved (12, 39, 40). Another possibility is the transient presence of some molecular mediator or pathway that interacts with the β4 auxiliary unit of the BK channel, as has been reported for some proteins in the postsynaptic domain (41). While further investigations are required to fully understand the contribution of presynaptic BK channels to regulate short vs long-term synaptic plasticity, it has been suggested that synaptic plasticity mechanisms have been implicated to synaptic maturation and circuitry formation (42). Particularly, LTD has been related to structural changes and a decrease in synaptic contacts (43, 44). Thus, a functional relevance of this BK-mediated plasticity can be related to the circuitry wiring, where LTD has been associated with pruning and a decrease in synaptic contacts (43, 44). Thus, synaptic plasticity could be relevant for establishing the hippocampal circuit, and BK channels could play a key role in its development, acting as a frequency filter, allowing high transmission rates to propagate but suppressing synapses that rely on low rates of transmission. In this way, BK channels may drive neuronal wiring in early development by enabling active synapses to undergo synaptic potentiation. However, whether BK channels' contribution to synaptic plasticity plays a role in synaptic wiring requires further investigations.

Materials and Methods

Hippocampal Slice Electrophysiology. Wild-type (WT) and TRPV1 null mice ($TRPV1^{-/-}$) were raised in the animal facility of the Universidad de Valparaiso and held at 20 to 25 °C under a 12-h light/dark cycle with water and food ad libitum. Animal handling and use followed a protocol approved by the bioethics committee of the Universidad de Valparaiso (CBC39/2022), in accordance with the bioethics and biosafety regulation of the Chilean Research Council (CONICYT).

Acute transverse hippocampal slices (400 μm thick) were prepared from Postnatal day (P) 7 to P13 mice of either gender as previously described (45, 46). Briefly, hippocampi were isolated and cutting using a DKT or Leica TS1200 vibratome in a solution containing the following (in mM): 215 sucrose, 2.5 KCl, 26 $NaHCO_3$, 1.6 NaH_2PO_4, 1 $CaCl_2$, 4 $MgCl_2$, 4 $MgSO_4$, and 20 glucose. After 30-min recovery, slices were incubated in an artificial CSF (ACSF) recording solution containing the following (in mM): 124 NaCl, 2.5 KCl, 26 $NaHCO_3$, 1 NaH_2PO_4, 2.5 $CaCl_2$, 1.3 $MgSO_4$, and 10 glucose equilibrated with 95% O_2/5% CO_2, pH 7.4. Slices were incubated for 30 min before recordings.

All experiments, except where indicated, were performed at 28 ± 1 °C in a submersion-type recording chamber perfused at 1 to 2 mL/min rate with ACSF supplemented with the $GABA_A$ receptor antagonist picrotoxin (PTX; 50 μM). Extracellular field potentials (fEPSPs) were recorded with a patch pipette filled with 1 mM NaCl and placed in the CA1 stratum radiatum (100 μm deep). Whole-cell voltage-clamp recordings (Multiclamp 700B Molecular Devices, USA) were made from CA1 pyramidal neurons voltage-clamped at −60 mV using patch-type pipette electrodes (3 to 4 M) containing the following intracellular solution (in mM): 131 Cs-gluconate, 8 NaCl, 1 $CaCl_2$, 10 EGTA, 10 glucose, 10 HEPES, pH 7.2, and 292 mmol/kg osmolality. For current clamp experiments, CA1 pyramidal neurons were recorded using a KCl-based intracellular solution (in mM): 130 KCl, 5 NaCl, 1 $MgCl_2$, 0.2 EGTA, 10 HEPES, 2 MgATP, and 0.1 NaGTP (adjusted to pH 7.2 with KOH).

fEPSPs and EPSCs were evoked by stimulating Schaffer collateral inputs with a monopolar electrode filled with ACSF and positioned ~100 to 150 μm away from the recording pipette. Two pulses (100 ms interstimulus interval) were used to calculate PPR that was defined as the ratio of the slope or amplitude of the second EPSP/EPSC to the slope or amplitude of the first EPSP/EPSC, respectively. The coefficient of variation ($1/CV^2$) was calculated as the squared mean EPSP/EPSC slope/amplitude divided by EPSP/EPSC variance. Both PPR and 1/CV were calculated 10 min before and 15 to 20 min after application of the LTD induction protocol. mGluR-LTD was evoked using a standard low-frequency stimulation (5 Hz, 900 pulses, 3 min) as previously described (2) or by bath application of 50 mM DHPG, a specific mGluR agonist. LFS- or DHPH-induced LTD was typically induced after 10 min of stable baseline and the magnitude of mGluR-LTD was compared 30 to 40 min after LTD protocol in the absence or presence of the pharmacological agents. In some experiments (Fig. 4*A*), puff application of L-glutamate (1 mM, 25 ms, 1 to 2 PSI bar) onto CA1 pyramidal neurons was delivered while neurons were voltage clamped at −60 mV. Reagents were obtained from Sigma, Tocris, and Ascent Scientific, prepared in stock solutions (water or DMSO), and added to the ACSF as needed. Total DMSO in the ACSF was maintained less than 0.01%. For whole cell experiments, series resistance (range, 8 to 12 MΩ) was monitored throughout the experiment with a 5 mV, 80 ms voltage step, and cells that exhibited significant change in series resistance (>20%) were excluded from analysis. Data were elicited at 15 to 20-s intervals, filtered at 2.2 kHz, and acquired at 10 kHz using a custom-made routine written in Igor Pro 6.37 (WaveMetrics, Portland, OR), whereas statistical comparisons were made using paired Student's *t* test at $P < 0.05$ significance level, using Origin 8.5 Pro software (OriginLab).

Channel Expression and Recordings. BK channels were expressed in *X. laevis* oocytes. The cDNA coding for the WT human BK α -subunit (Gen bank U11058), the human β_2-subunit (Gen bank AF099137) without inactivation domain (β_2IR) (47), and β_4-subunit (Gen Bank AF160967) were provided by L. Toro (University of California, Los Angeles, CA). The mRNA was prepared in vitro by using the mMESSAGE mMACHINE (Ambion) kit. The oocytes were injected with 50 ng of mRNA and incubated in an ND96 solution (96 mM NaCl, 2 mM KCl, 1.8 mM $CaCl_2$, 1 mM $MgCl_2$, and 5 mM HEPES, pH adjusted to 7.4 with NaOH) at 18 °C for 3 to 5 d before electrophysiological recordings. All the recordings were acquired by using the patch-clamp technique in the inside-out configuration. Data were acquired with an Axopatch 200B (Molecular Devices) amplifier and the Clampex 10 (Molecular Devices) acquisition software. Both, the voltage command, and current output were filtered at 10 kHz with an 8-pole Bessel low-pass filter (Frequency Devices). Current signals were sampled with a 16-bit A/D converter (Digidata 1550B; Molecular Devices), using a sampling rate of 500 kHz. Unless otherwise stated, linear membrane capacitance and leak subtraction were performed based on a P/-8 protocol (48). Borosilicate capillary glasses (1B150F-4, World Precision Instruments) were pulled in a horizontal pipette puller (Sutter Instruments). After fire-polishing, pipette resistance was typically 1 to 2 MΩ. An agar bridge with Cl^- as the main anion was used as the ground electrode. All experiments were performed at room temperature (18 to 20 °C).

Postassium currents (I_K) were elicited by 10-ms voltage steps of 10 mV, except for $\alpha + \beta_2$IR or $\alpha + \beta_4$ channel currents, that were elicited by 40-ms pulse durations. The holding voltage was -100 mV for all channels and the final voltage was 300 mV. The pipette and bath solutions were almost the same and typically contained 110 mM KOH, 10 mM HEPES, and 5 mM EGTA (free Ca^{2+} ~0.8 nM) (49), while the pipette external solution contained extra 2 mM $MgCl_2$. The pH for both cases was adjusted to 7.4 with about 108 mM $HMeSO_3$. For test solutions using Ca^{2+} (3 μM), $CaCl_2$ was added to reach the desired free [Ca^{2+}], and 2 mM EGTA was used as calcium buffer. Free calcium concentration was estimated using the WinMaxChelator Software and checked with a Ca^{2+}-electrode (Hanna Instruments).

Data Analysis. For ionic current experiments, the instantaneous $I_{tail,i}(V)$ data for each *i* experiment were fitted by using a Boltzmann function,

$$I_{tail,i}(V) = \frac{I_{tail,i,max}}{1 + e^{\left(\frac{-z\delta F\left(V - V_{h,i}\right)}{RT}\right)}}(X),$$

where $I_{tail,max}$ is the maximum tail current, $z\delta$ is the voltage dependency for channel activation, V_h is the half-activation voltage, T is the absolute temperature (294 K), F is the Faraday's constant, and R is the universal gas constant. The best values for $I_{tail,max}$, V_h, and $z\delta$ were determined by using the Matlab´s function *lsqnonlin*. The averaged half activation voltage ($< V_h >$) and the averaged voltage dependency ($< z\delta >$) were reported as mean ± SEM of the *n* experiments. Each individual $I_{tail,i}(V)$ curve was normalized by dividing by its specific $I_{tail,i,max}$ value and then aligned by shifting along the voltage axis by $\left(< V_h > - V_{h,i} \right)$. A further shift of the $I_{tail,i}(V)$ curves was done by rounding each voltage value to the nearest ten. This procedure allowed generating an averaged $I_{tail,i}(V)$ curve with a voltage dependence representative of the *n* experiments (50).

Data, Materials, and Software Availability. All study data are included in the article and/or *SI Appendix*.

ACKNOWLEDGMENTS. This work was supported by the Chilean government through FONDECYT Regular #1201848 (A.E.C.), #1230265 (R.L.), #1171840 (C.Q.C.), ANID Millennium Science Initiative Program (P09-022F to R.L, C.Q.C., and A.E.C.), and the National Institute Award RO1GM030376 (R.L.). C.A.-G. and A.A. were supported by PhD fellowship from ANID #21201603 (C.A.-G.) and #21202136 (A.A.). R.C.M. was supported by ANID-FONDECYT postdoctorado Grant #3190793.

Author affiliations: [a]Programa de Doctorado en Ciencias Mención Neurociencia, Facultad de Ciencias, Universidad de Valparaíso, Valparaíso 2340000, Chile; and [b]Instituto de Neurociencias, Centro Interdisciplinario de Neurociencia de Valparaíso, Facultad de Ciencias, Universidad de Valparaíso, Valparaíso 2340000, Chile

1. C. Luscher, K. M. Huber, Group 1 mGluR-dependent synaptic long-term depression: Mechanisms and implications for circuitry and disease. *Neuron* **65**, 445–459 (2010).
2. S. J. Feinmark *et al.*, 12-lipoxygenase metabolites of arachidonic acid mediate metabotropic glutamate receptor-dependent long-term depression at hippocampal CA3-CA1 synapses. *J. Neurosci.* **23**, 11427–11435 (2003).
3. V. Y. Bolshakov, S. A. Siegelbaum, Postsynaptic induction and presynaptic expression of hippocampal long-term depression. *Science* **264**, 1148–1152 (1994).
4. V. Y. Bolshakov, S. A. Siegelbaum, Regulation of hippocampal transmitter release during development and long-term potentiation. *Science* **269**, 1730–1734 (1995).
5. R. C. Hardie, TRP channels and lipids: From *Drosophila* to mammalian physiology. *J. Physiol.* **578**, 9–24 (2007).
6. F. J. Taberner *et al.*, TRP channels interaction with lipids and its implications in disease. *Biochim. Biophys. Acta* **1848**, 1818–1827 (2015).
7. H. E. Gibson *et al.*, TRPV1 channels mediate long-term depression at synapses on hippocampal interneurons. *Neuron* **57**, 746–759 (2008).
8. L. M. Boland, M. M. Drzewiecki, Polyunsaturated fatty acid modulation of voltage-gated ion channels. *Cell Biochem. Biophys.* **52**, 59–84 (2008).
9. M. L. Roberts-Crowley *et al.*, Regulation of voltage-gated Ca^{2+} channels by lipids. *Cell Calcium* **45**, 589–601 (2009).
10. A. Besana, R. B. Robinson, S. J. Feinmark, Lipids and two-pore domain K^+ channels in excitable cells. *Prostaglandins Other Lipid Mediat.* **77**, 103–110 (2005).
11. M. Carta *et al.*, Membrane lipids tune synaptic transmission by direct modulation of presynaptic potassium channels. *Neuron* **81**, 787–799 (2014).
12. C. Ancaten-Gonzalez *et al.*, Ca(2+)- and voltage-activated K(+) (BK) channels in the nervous system: One gene, a myriad of physiological functions. *Int. J. Mol. Sci.* **24**, 3407 (2023).
13. J. R. Montgomery, A. L. Meredith, Genetic activation of BK currents in vivo generates bidirectional effects on neuronal excitability. *Proc. Natl. Acad. Sci. U.S.A.* **109**, 18997–19002 (2012).
14. M. H. Zink *et al.*, 12-lipoxygenase in porcine coronary microcirculation: Implications for coronary vasoregulation. *Am. J. Physiol. Heart Circ. Physiol.* **280**, H693–H704 (2001).

15. F. M. Faraci *et al.*, Arachidonate dilates basilar artery by lipoxygenase-dependent mechanism and activation of K(+) channels. *Am. J. Physiol. Regul. Integr. Comp. Physiol.* **281**, R246–R253 (2001).
16. H. Hu *et al.*, Presynaptic Ca^{2+}-activated K^+ channels in glutamatergic hippocampal terminals and their role in spike repolarization and regulation of transmitter release. *J. Neurosci.* **21**, 9585–9597 (2001).
17. H. Misonou *et al.*, Immunolocalization of the Ca^{2+}-activated K^+ channel Slo1 in axons and nerve terminals of mammalian brain and cultured neurons. *J. Comp. Neurol.* **496**, 289–302 (2006).
18. G. Raffaelli *et al.*, BK potassium channels control transmitter release at CA3-CA3 synapses in the rat hippocampus. *J. Physiol.* **557**, 147–157 (2004).
19. C. A. Sailer *et al.*, Immunolocalization of BK channels in hippocampal pyramidal neurons. *Eur. J. Neurosci.* **24**, 442–454 (2006).
20. V. Y. Bolshakov, S. A. Siegelbaum, Hippocampal long-term depression: Arachidonic acid as a potential retrograde messenger. *Neuropharmacology* **34**, 1581–1587 (1995).
21. S. S. Zakharenko, L. Zablow, S. A. Siegelbaum, Altered presynaptic vesicle release and cycling during mGluR-dependent LTD. *Neuron* **35**, 1099–1110 (2002).
22. M. Normandin *et al.*, Involvement of the 12-lipoxygenase pathway of arachidonic acid metabolism in homosynaptic long-term depression of the rat hippocampus. *Brain Res.* **730**, 40–46 (1996).
23. C. A. Rice, R. W. Stackman Jr., The small conductance Ca(2+)-activated K(+) channel activator GW542573X impairs hippocampal memory in C57BL/6J mice. *Neuropharmacology* **252**, 109960 (2024).
24. R. Brenner *et al.*, BK channel beta4 subunit reduces dentate gyrus excitability and protects against temporal lobe seizures. *Nat. Neurosci.* **8**, 1752–1759 (2005).
25. C. Contet *et al.*, BK channels in the central nervous system. *Int. Rev. Neurobiol.* **128**, 281–342 (2016).
26. J. Zhang *et al.*, Glutamate-activated BK channel complexes formed with NMDA receptors. *Proc. Natl. Acad. Sci. U.S.A.* **115**, E9006–E9014 (2018).
27. Y. Zhou, C. J. Lingle, Paxilline inhibits BK channels by an almost exclusively closed-channel block mechanism. *J. Gen. Physiol.* **144**, 415–440 (2014).
28. P. E. Castillo *et al.*, Endocannabinoid signaling and synaptic function. *Neuron* **76**, 70–81 (2012).
29. W. G. Regehr, M. R. Carey, A. R. Best, Activity-dependent regulation of synapses by retrograde messengers. *Neuron* **63**, 154–170 (2009).
30. Y. Wu *et al.*, TRPV1 channels are functionally coupled with BK(mSlo1) channels in rat dorsal root ganglion (DRG) neurons. *PLoS ONE* **8**, e78203 (2013).
31. M. S. Hunsberger, M. Mynlieff, BK potassium currents contribute differently to action potential waveform and firing rate as rat hippocampal neurons mature in the first postnatal week. *J. Neurophysiol.* **124**, 703–714 (2020).
32. P. Y. Deng *et al.*, FMRP regulates neurotransmitter release and synaptic information transmission by modulating action potential duration via BK channels. *Neuron* **77**, 696–711 (2013).
33. S. Shruti *et al.*, The brain-specific Beta4 subunit downregulates BK channel cell surface expression. *PLoS ONE* **7**, e33429 (2012).
34. L. R. Shao *et al.*, The role of BK-type Ca^{2+}-dependent K^+ channels in spike broadening during repetitive firing in rat hippocampal pyramidal cells. *J. Physiol.* **521**, 135–146 (1999).
35. T. Hoshi *et al.*, Mechanism of the modulation of BK potassium channel complexes with different auxiliary subunit compositions by the omega-3 fatty acid DHA. *Proc. Natl. Acad. Sci. U.S.A.* **110**, 4822–4827 (2013).
36. A. M. Dopico, A. N. Bukiya, Lipid regulation of BK channel function. *Front. Physiol.* **5**, 312 (2014).
37. J. T. King *et al.*, Beta2 and beta4 subunits of BK channels confer differential sensitivity to acute modulation by steroid hormones. *J. Neurophysiol.* **95**, 2878–2888 (2006).
38. T. Zaman *et al.*, BK channels mediate synaptic plasticity underlying habituation in rats. *J. Neurosci.* **37**, 4540–4551 (2017).
39. A. G. Leenders, Z. H. Sheng, Modulation of neurotransmitter release by the second messenger-activated protein kinases: Implications for presynaptic plasticity. *Pharmacol. Ther.* **105**, 69–84 (2005).
40. P. E. Castillo, Presynaptic LTP and LTD of excitatory and inhibitory synapses. *Cold Spring Harb. Perspect. Biol.* **4**, a005728 (2012).
41. C. Lohmann, H. W. Kessels, The developmental stages of synaptic plasticity. *J. Physiol.* **592**, 13–31 (2014).
42. S. Chaudhury *et al.*, Activity-dependent synaptic plasticity modulates the critical phase of brain development. *Brain Dev.* **38**, 355–363 (2016).
43. N. Becker *et al.*, LTD induction causes morphological changes of presynaptic boutons and reduces their contacts with spines. *Neuron* **60**, 590–597 (2008).
44. C. Piochon, M. Kano, C. Hansel, LTD-like molecular pathways in developmental synaptic pruning. *Nat. Neurosci.* **19**, 1299–1310 (2016).
45. A. E. Chavez, C. Q. Chiu, P. E. Castillo, TRPV1 activation by endogenous anandamide triggers postsynaptic long-term depression in dentate gyrus. *Nat. Neurosci.* **13**, 1511–1518 (2010).
46. A. E. Chavez *et al.*, Compartment-specific modulation of GABAergic synaptic transmission by TRPV1 channels in the dentate gyrus. *J. Neurosci.* **34**, 16621–16629 (2014).
47. M. Wallner, P. Meera, L. Toro, Molecular basis of fast inactivation in voltage and Ca^{2+}-activated K^+ channels: A transmembrane beta-subunit homolog. *Proc. Natl. Acad. Sci. U.S.A.* **96**, 4137–4142 (1999).
48. C. M. Armstrong, F. Bezanilla, Currents related to movement of the gating particles of the sodium channels. *Nature* **242**, 459–461 (1973).
49. D. H. Cox, J. Cui, R. W. Aldrich, Separation of gating properties from permeation and block in MSLO large conductance Ca-activated K^+ channels. *J. Gen. Physiol.* **109**, 633–646 (1997).
50. F. T. Horrigan, R. W. Aldrich, Coupling between voltage sensor activation, Ca^{2+} binding and channel opening in large conductance (BK) potassium channels. *J. Gen. Physiol.* **120**, 267–305 (2002).